

Enhancement of a green supercapacitor with a hydrogel/carbon nanotubes-based electrolyte

Marquidia Pacheco, Member, IEEE, María Fernanda Monroy, Alfredo Santana-Díaz, Joel Pacheco, Ricardo Valdivia-Barrientos, Xin Tu, Senior Member, IEEE, Alberto González-Pedroza, and María Teresa Ramírez-Palma

Abstract— The purpose of this work is to suggest the conception of a supercapacitor using environment-friendly materials, in addition to exhibiting good electrochemical performances. In order to lower the environmental footprint of supercapacitors, one current attempt in the literature is to replace efficient but toxic organic electrolytes by harmless, bio-friendly electrolytes such as a mixture of sodium salt with a hydrogel. However, those bio-friendly electrolytes have not been demonstrated yet to be a relevant alternative, as they are still not able of similar performances as toxic organic electrolytes. The work reported in this paper demonstrates, as a different approach, that the capacitance of a bio-friendly, hydrogel-based electrolyte combined with sodium salt can be significantly increased by adding carbon nanotubes (CNTs) to the gel. As a result, the supercapacitor using the CNT-loaded bio-friendly electrolyte has registered not only an enhanced capacitance, but also better energy and power densities compared to both the same but CNT-free electrolyte, and a toxic DMSO-based organic electrolyte.

Index Terms— Energy storage, supercapacitors, nanotechnology, nanotubes.

Manuscript received August 3, 2020; accepted August 24, 2020. This work was supported in part by CONACyT-SENER under Grant 245225 and in part by the project AM608 ININ. The review of this article was arranged by Associate Editor Prof. Chi Zang. (Corresponding author: Marquidia Pacheco)

Marquidia Pacheco, Joel Pacheco and Ricardo Valdivia are with the Instituto Nacional de Investigaciones Nucleares (ININ), 52750, México (e-mail: marquidia.pacheco@inin.gob.mx, joel.pacheco@inin.gob.mx, ricardo.valdivia@inin.gob.mx).

M. Monroy is with the ININ and with the Engineering Faculty of the Universidad Autónoma del Estado de México (UAEM), 50130, México (e-mail mfer.monroy@gmail.com).

Alfredo Santana-Díaz is with the Instituto Tecnológico y de Estudios Superiores de Monterrey, 50110, Mexico (e-mail: asantana@tec.mx).

Xin Tu is with Department of Electrical Engineering and Electronics, University of Liverpool, Liverpool L69 3GJ, U.K. (e-mail: xin.tu@liverpool.ac.uk).

Alberto González-Pedroza is with the ININ, and also with Instituto Tecnológico de Toluca, 52149 Metepec, Mexico (e-mail: albertoglezjp@gmail.com).

María Teresa Ramírez-Palma is with Engineering Faculty, (UAEM), 50130, Mexico (e-mail: rmarytere@yahoo.com.mx).

Digital Object Identifier 10.1109/TNANO.2020.3019764

I. INTRODUCTION

TWO of the most important characteristics to enhance electrochemical properties on supercapacitors are the surface area of the electrodes-electrolyte interface and the electrolyte itself.

To increase the surface area, porous materials have been widely used; particular attention has been dedicated on carbon nanostructures; besides their high surface area (up to 1300 m²/g), their covalent sp² bond between individual carbon atoms provides high electrical conductivity [1].

Concerning the electrolytes, they could have a strong influence on the energy density (i.e. the energy density is proportional to the square of the cell voltage).

In general, aqueous electrolytes have high conductivity and capacitance but their working voltage is limited, whereas organic electrolytes can operate at higher voltages, but they normally suffer from lower ionic conductivity.

Aqueous based electrolytes have an operational potential window of about 1 to 1.3V, whereas organic electrolyte-based and ionic liquids respectively have potential windows of 2.5–2.7V and 3.5–4.0 V [2]; these higher potential windows directly influence on the increase of the capacitance. These electrolytes are generally composed of hazardous materials, such as strong acids or alkalines, or organic solvents like the dimethylsulfoxide (DMSO) [3].

Furthermore, concerning the ionic liquids, the commonly used anions contain halogen fluoro-complex salts are not only expensive, but they can be hydrolyzed to generate hydrogen fluoride in the presence of a trace of water [4].

Likewise, the use of liquids makes the supercapacitor heavier and there exists the possibility of electrolyte leakages, so the use of gel electrolytes could be interesting to avoid these drawbacks. Additionally, the surface of solid or semisolid systems can improve the ionic transport ability [5], and the specific capacitance augments when viscosity of the electrolyte increases [6].

Taking into account the drawbacks previously mentioned, the use of gel electrolytes with harmless materials is an interesting field to explore. In particular hydrogels can present advantages like ease of processing, larger electrochemically surface area, shortened pathways for mass transport and lower

cost compared with “traditional” devices [6-8].

The supercapacitor device here used was then inspired by previous works cited. A polysaccharide-based hydrogel, in particular sodium alginate was chosen because some properties such as flexibility and high cycling performance [9]. The alginates are a family of water-soluble polymers extracted from brown seaweed, like sargassum. The Caribbean region has seen an explosion in Sargassum densities with unusually high extent; some scientists have linked this disaster with global climate change [10]. From these facts, the use of alginate to assemble supercapacitors could provide an additional advantage such as low cost of raw material. Furthermore, the sodium alginate with conductive particles, such as CNT, has good mechanical strength attributed to the intermolecular and intramolecular hydrogen bonding between SA chains, and to the attractive electrostatic force inside the entanglement among SA chains and the carbon nanostructure [7].

In particular, in this work the neutral aqueous electrolyte NaCl, was suggested because it could improve performance of carbon nanoparticulates in supercapacitors. The size of its hydrous cation Na^+ is small and combined with its small monoion Cl^- , could improve capacitances, mostly at high potential scan rate. Additionally, the effect of nanoparticulates with those electrolytes at relatively high temperatures (i.e 30-60°C) could also increase capacitance [11].

The necessity of using innocuous materials and, at the same time, having good electronic properties such as shorts times of charge/discharge and high capacitance are qualities of ideal supercapacitors. In this work we intend to combine those characteristics; specifically, a biohydrogel mixed with carbon nanotubes (CNT) in a micromembrane to augment the superficial area; the influence different electrolytes will be also studied in order to determine the best electrolyte for the supercapacitor configuration.

II. EXPERIMENTAL

A. Supercapacitor device assembly

The supercapacitor device is formed by 2 copper foils of 1.5cm x 1.5cm acting as electrodes and two types of separators, the first one made with a micromembrane impregnate with sodium alginate, dimethylsulfoxide (DMSO) and ethanol (SA), and the second one made with a micromembrane impregnate with sodium alginate and sodium chloride (NaCl).

In order to increase the capacitance for all configurations carbon nanotubes (CNT) were added; they could increase the conductive properties and the surface area of the supercapacitor. In order to provide an approach of the bonding between the different compounds used, a Fourier Transform Infrared (FTIR) analysis was realized.

B. Electrolytic gel preparation

For the Configuration 1, 1.002 g of CNT are mixed with the SA solution (1ml); the micromembrane is then deposited and it is posteriorly placed in an ultrasonic bath for 2 hours. For Configuration 2 and Configuration 3, the electrolytic solutions are added to the previous mixture; those solutions respectively were 0.5ml DMSO/0.5ml Ethanol and 1ml of NaCl 0.1M. In particular, NaCl was chosen because neutral electrolytes have advantages such as larger working potential windows, less corrosion and greater safety [2]. Finally, 1 ml of calcium chloride (CaCl) is added to the imbibed membrane in order to form the biohydrogel.

A schema of the supercapacitor assembly is represented in Fig. 1. CNT used are mostly singlewalled nanotubes (Fig. 2a). Those nanotubes were obtained from electric arc technique using the method described in [12] using a mixture of nickel and yttrium as catalysts.

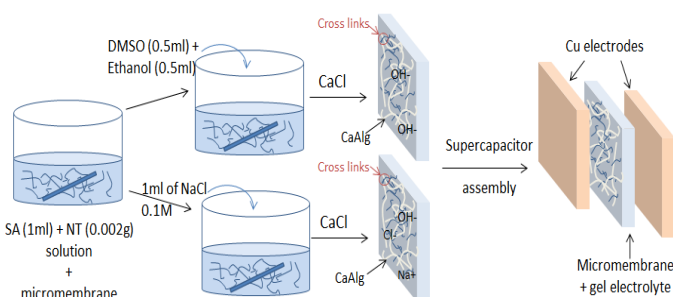
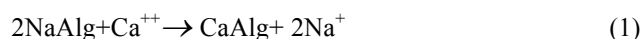


Fig. 1. Schematic representation of the supercapacitor assembly. When the solutions of *DMSO+Ethanol+SA+NT* and *NaCl+water+SA+NT* enter in contact with *CaCl* the gel is formed. The micromembrane impregnated with the gel is placed between two Cu electrodes.

Alginate gel is formed when SA solution is in contact with calcium chloride solution. The SA becomes alginate of calcium and sodium ions are then released, following the chemical reaction described in Eq. (1) [13].



Initially the center is constituted of unreacted sodium alginate (NaAlg), and over a period of time the calcium ion (Ca^{++}) will diffuse into the center and form a complete calcium structure (CaAlg) and sodium ions (Na^+) [14].

The different configurations of membranes (Fig. 2b) are placed between the copper electrodes, this system is then placed in a container (yellow box in Fig. 2b) allowing a uniform distance between electrodes to obtain a correct measurement.

C. Electrochemical characterization of the supercapacitor device

In this study all the experiments were realized in the potentiostat/galvanostat with a two cell electrode configuration. It has been studied that three-electrode cells differ from two-electrode measurements; the amplified sensitivity of the first one can lead to large errors when

projecting the energy storage capability of an electrode material for supercapacitor use [15].

The electrochemical characterization was realized using cyclic voltammetry, galvanostatic charge-discharge and electrochemical impedance spectroscopy. To obtain current-voltage (C-V) tests a potential window of 0 to 1V was used at two scan rates 0.05Vs^{-1} and 0.1Vs^{-1} at 10mA. Impedance data were collected from 100kHz to 0.1Hz.

III. THEORY

From the C-V graphs, the specific capacitance (C_{sp}) could be obtained following the Eq (2) [14]:

$$C_{sp} = \frac{2 \int idV}{\Delta V v \cdot m} \quad (2)$$

Where:

C_{sp} : mass specific capacitance (Fg^{-1})

$\int idV$: Surface area of the C-V graph (VA)

v : Scan rate (Vs^{-1})

ΔV : Potential window (V)

m : Weight of the carbon material in the electrode layer

(g).

In a symmetrical two-electrode cell the potential differences applied to each electrode are equal to each other and are one half of the values shown on the X-axis of the C-V diagram [16]. Therefore, the factor of 2 accounts for the two-electrode setup, assuming a homogeneous distribution of the charge.

The energy density (E_{sp}) and the power density (P_{sp}) of the supercapacitor, could respectively be obtained with Eq. (3) and Eq.(4)

$$E_{sp} = \frac{1}{2} C_{sp} V^2 \quad (3)$$

$$P_{sp} = \frac{1}{4mR_{cell}} V^2 \quad (4)$$

Where:

V : cell voltaje (V).

R_{cell} : is the equivalent series resistance of the supercapacitor cell (Ω).

The equivalent series resistance of the supercapacitor cell (R_{cell}) is also known as the internal resistance defined as the sum of the resistances of the electrolyte including the separator, the current collector, and the contact resistance between the electrode and the current collector (porous layer) [17].

The calculus of R_{cell} could be made from circuit models obtained from the fitting of Nyquist plots; however, those models have some limitations because one unique value of R_{cell} can be founded with two or more circuit models using different configurations of ideal capacitors and resistors [18].

In addition, those circuit models do not take into account neither the ion diffusion nor the heterogeneity of ion concentrations in the electrolyte [19].

To overcome these drawbacks, some researchers [20] have developed a physicochemical transport model considering the electric double layer, the charge transport in the electrode and the ion electro-diffusion. From this model it is possible to obtain the internal resistance in the Nyquist plot and corresponds to the value of the real part of the electrochemical impedance at the end of the semicircle, normally formed at high frequencies, just before the steep slope corresponding to diffuse layer resistance at intermediate frequencies, as schematized in Fig. 2.

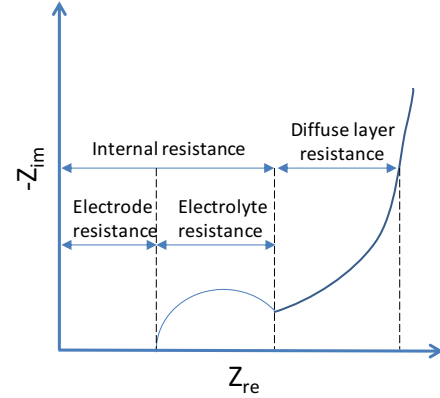


Fig. 2 Typical Nyquist plot where the equivalent series resistance corresponds to value at the end of the semicircle, according to [20].

The differential capacitance C_{Diff} at a scan rate (v) constant could be expressed as follows:

$$C_{Diff} = \frac{dQ}{dV} = \frac{i(V)}{v} \quad (5)$$

Where:

Q : Electric charge

Differential capacitance was computed with Simulink® by supposing that the supercapacitor is totally charged. The power source is then, cut off, and the capacitor is discharged by help of an electronic load at a constant current.

IV. RESULTS AND DISCUSSION.

A. FTIR and XPS Spectra

The results of the FTIR analysis are shown in Fig. 3c. It could be seen that for the three cases, there is a broad absorption band at around 3200cm^{-1} , corresponding to stretching vibrations of O-H, since the alginate is mainly composed of this type of strong bonds. Likewise, there is an absorption band between 2800cm^{-1} and 3000cm^{-1} , where C-OH stretching vibrations are found, that could indicate strong bonds between the carbon structures and the alginate.

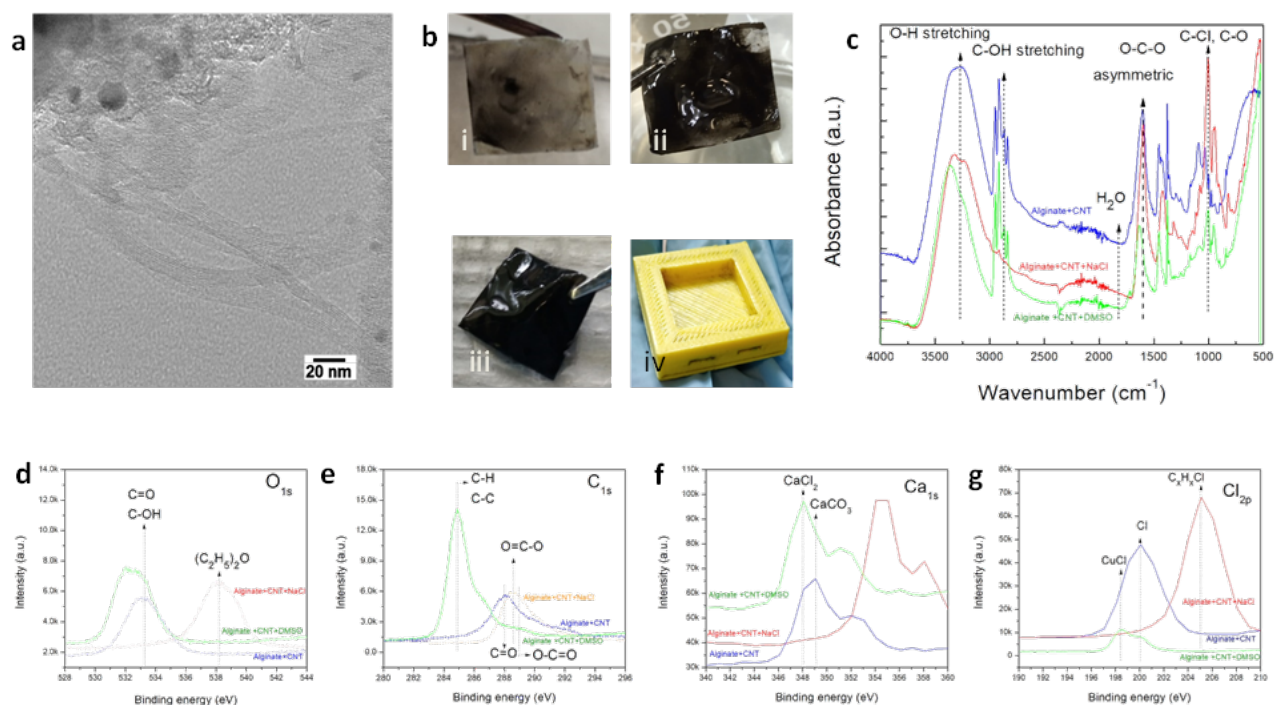


Fig. 3. Different CNT membranes of the supercapacitor and their respective FTIR spectra and XPS analysis. **a** Single walled nanotubes used in all configurations, **bi** Membrane with alginate + CNT + NaCl, **bii** Membrane with Alginate + CNT + DMSO/Ethanol, **biii** Membrane with Alginate + CNT + NaCl, **biv** Supercapacitor container, **c** FTIR Spectra, **d** to **g** XPS spectra.

There are also absorption bands ranging from 1600cm^{-1} to 875cm^{-1} , which indicate deformations, stretches and torsions in the carbonyl groups. Among them asymmetric O-C-O (carboxylate) vibrations with a peak at around 1580cm^{-1} , a peak near to 1410cm^{-1} corresponding to O-C-O symmetric vibrations, and C-Cl and C-O links at around 1000cm^{-1} and at 1100cm^{-1} . Similar results were obtained by [10] there have obtained similar deformations and stretching, so it can be said that, for the three electrolytes, most of the bonds are due to alginate and carbon nanostructures; although in the case of C3 the links are mostly due to the O-H bond, while in C1 and C2 there is a combination between O-H and C-OH bonds.

A comparison of C_{1s} and O_{1s} XPS spectra could be seen respectively in Fig 3.b and in Fig 3.e. From these figures we can deduce that CNT have influence on electrolytes because some links between carbon and oxygen were obtained. The bonds are mainly with hydrogen, carbon and oxygen, which are attributed to the composition of alginate [9] and alginate in combination with the CNT. Interaction of the biohydrogel and the sodium electrolyte could be deduced from Fig. 3.f, where links of Ca_{1s} and Cl_{2p} can be seen. The interaction of C with Cu from the electrodes when DMSO is used as electrolyte is observed in Fig. 3 g.

B. Cyclic voltammetry measurements

The CV curves obtained for three configurations at 0.1Vs^{-1} and 0.05Vs^{-1} could be respectively observed in Fig. 4a and Fig. 4b. From these figures larger areas of the C-V curves are obtained with Alginate + CNT + NaCl. Furthermore, at lower scan rates (i.e 0.05Vs^{-1}) higher capacitances are obtained for three configurations. However, it is important to note that the diminution of scan rates does not necessarily implies the increase of the C-V curve area; as example, opposing results have been obtained in [21] and in [22]. In those cases, the C-V area was directly proportional to the scan rate. So, in the conditions here presented, the scan rate of 0.05Vs^{-1} is enough to facilitate a correct transit of ions between both electrodes.

C. Galvanostatic charge-discharge and stability studies

The curve of charge and discharge time is shown in Fig. 3c; similar behavior was obtained for three configurations.

Galvanostatic curves present symmetrical shapes indicating capacitive characteristics nearly to ideal behavior. The use of NaCl certainly allows a free diffusion, and then, a faster diffusion of hydrated Na^+ and Cl^- ions inside the biopolymer matrix, as reported by [23]. In particular, they used NaCl as a dopant to improve the supercapacitor properties.

For the Configuration 1 (Alginate + CNT) 900 cycles were reached during 4.8h, the Configuration 2 (Alginate +CNT+ DMSO/Ethanol) reached 1000 cycles through 6.9h and the Configuration 3 (Alginate + CNT + NaCl) attain around 800 cycles in 5.6h. So the endurance of the supercapacitor could be enhanced with the addition of DMSO. Compared to data reported in [23], the Configuration 3 here proposed, displays

relatively low long-term cycle stability. In [23] they were able to reach 4.7 h over 900 charge–discharge cycles with a NaCl-doped gelatin hydrogel electrolyte.

One possible explanation of this behavior could be the NaCl concentration. The NaCl concentration used in [23] is superior (i.e 3N) than that used in this work. Therefore, at higher concentrations of the electrolyte the ionic conductivity increases because to the increased charge carrier concentration. As the current density increases, the time required to attain the cutoff voltage decreases, which affects formation of the electric double-layer, leading to an increase in the charge/discharge efficiency [24].

D. Electrochemical impedance spectroscopy

The Nyquist plots obtained from the study of electrochemical impedance spectroscopy are showed in Fig. 5d. The depressed semi-circle in the high frequency region is attributed to the Faradaic process of the charge exchange at the carbon/electrolyte interface [25]. Due to the semi-infinite diffusion of ions on carbon/ electrolyte interfaces, a straight line at low frequencies can be expressed by using a Warburg diffusion element [26] and a straight line with a slope of nearly 45° in the low frequency region, which is typical for the impedance spectra of porous films.

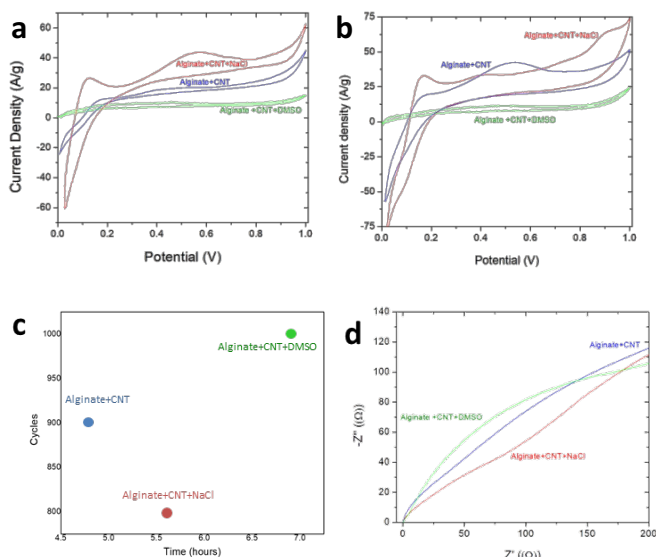


Fig 4. Cyclic voltammetry, galvanostatic charge/discharge and electrochemical impedance spectroscopy. **a** Cyclic voltammetry at 0.1Vs⁻¹, **b** Cyclic voltammetry at 0.05Vs⁻¹, **c** Number of cycles, **d** electrochemical impedance spectroscopy.

E. Capacitance, energy and power densities of the supercapacitor prototype

The behavior of differential capacitance during charge and discharge could be seen in Fig. 5. During charging time, the switch stays in position 1 (Fig. 5b) through 22s. C_{Diff} attains the value of 10F until the voltage across the supercapacitor is 12V; at this time, the switch passes to position 2 and a dynamic phenomenon begins with an increase of discharge current manifested by a negative impulsion at around 20A (blue line in figure 5c); simultaneously a sharp decreasing in

voltage from 12 to 7.3V (redline, section II) is revealed. For these new values C_{Diff} acquires a new value of 14F (section III in figure 5a).

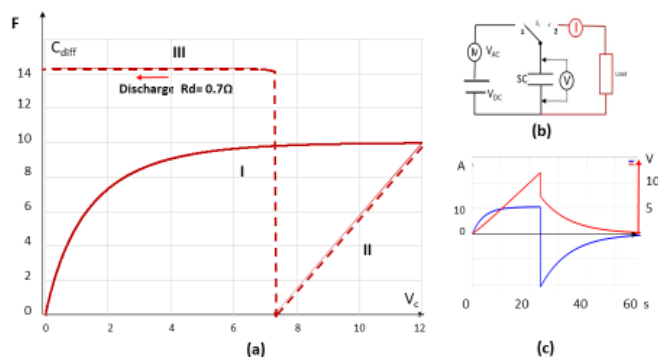


Fig 5. Differential capacitance in function of voltage during charge and discharge.

Results obtained from Eq. (2), Eq. (3) and Eq. (4) are summarized in Table I and Fig. 6. Under voltage windows of 0 to 1V the Configuration 3 (Alginate + CNT + NaCl) has higher values of capacitance, energy and power. This could be explained by the fact that organic electrolytes, such as DMSO (Configuration 2), have larger solvated ions sizes and lower dielectric constants, which can lead to lower capacitance values. These bigger ions could inhibit the transfer of Na^+ , the capacitances of prototypes using DMSO (Configuration 2) are even smaller than the prototype without electrolyte (Configuration 1), as can be observed in Fig. 4a and 4b.

Furthermore, the pseudo-capacitive contribution depends on the nature of carbon surfaces; this contribution requires an active proton participation; in particular, the DMSO is an aprotic organic electrolyte and then, the contribution of protons is poor [2].

Additionally, as reported in Table I, the capacitance value of the Configuration 3 (Alginate + CNT + NaCl) obtained in this work is, in general, superior to data reported in [5], [27] and [29-32]. It is important to mention that these references do not have the same experimental conditions (electrolytes, carbon nanostructures), however special caution has been taken into account to have the nearest experimental conditions.

It is worth to note that one capacitance value [28] could attain more than 3 times the values reported in Table I, including the results of the present work. Apparently, the use of PANI, additional to carbon nanostructures, could enhance the capacitance.

As detailed in [33] small nanoscaled and nanostructured PANI can reduce the diffusion length, enhance the electroactive regions, and further increase the capacitive performance of nanocomposites. An additional advantage of using PANI-SA is the increase of the hydrogel strength explained by the synergy of hydrogen bonds and van der Waals interactions between both compounds [34].

Likewise, by comparing results obtained in [32] and [33] the addition of SA clearly shows an important increase on capacitance, sodium and chloride ions in gel electrolyte have an important contribution. Particularly, the role of NaCl, as aqueous electrolyte, allows higher capacitance because those

electrolytes are composed of smaller ions as was reported in [34]. Another advantage of using NaCl as electrolyte could be explained by the small hydrous ionic radius of the cation Na^+ (i.e. 0.358nm) conjugated to the high capacity of anion Cl^- to highly dissolve in water; this anion could lead to a larger capacitance; NaCl allows to increase number of ions available to form the double layer at the electrolyte interface with the electrode [11].

Data of energy and power densities were taken from Table I and schematized on a Ragone plot (i.e Fig. 6).

The lower cell resistance for configuration 3 compared to other two configurations allow to have high power densities; however, as described before, it presents a relatively low charge-discharge. This could be explained by the fast migration of hydrated Na^+ and Cl^- ions between the electrodes leading to a faster damage of electrochemical supercapacitors [11].

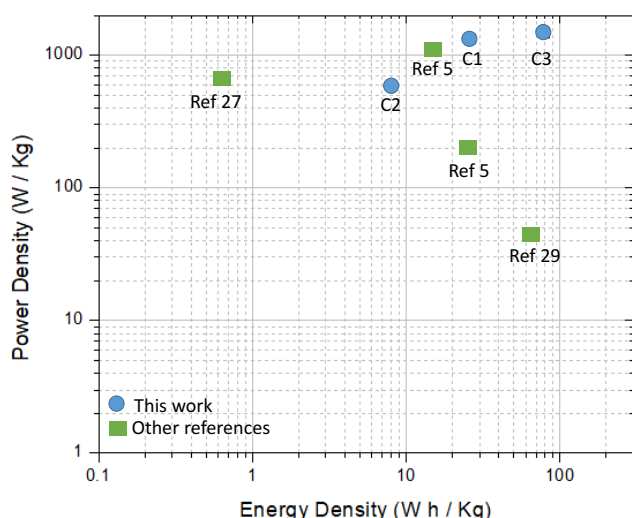


Fig.6. Ragone plot of diverse hydrogels. In blue circles the data reported in this work. In green squares the results from similar works.

Moreover, from the Fig.6 it is possible to observe better energy and power densities of the alginate over the agarose prototypes described in [5]. The molecules of both compounds are similar, as could be seen in Fig. 7.

Both molecular structures contain a large number of hydroxyl groups, facilitating their application as polyelectrolyte [7], besides both have intra and intermolecular hydrogen bonding and their porous structure enables high ratio of energy delivery [5] [7]. The Na insertion in SA, seems to act as an electrolytic channel.

And, finally, the use of CNT instead graphenes [29], or carbon nanosheets [31], seems to enhance the electrochemical properties of the supercapacitor device.

TABLE I
ELECTROCHEMICAL PERFORMANCE OF SUPERCAPACITORS COMPARED WITH OTHER WORKS
USING GEL ELECTROLYTES

Configuration	Capacitance density (F/g)	Energy density (W h kg^{-1})	Power density (W kg^{-1})
Alginate + CNT (C1)	188.1	26.24	1329.90
Alginate +CNT+ DMSO/ Ethanol (C2)	58.0	8.06	594.97
Alginate + CNT +NaCl (C3)	548.3	76.15	1474.82
Agarose gel electrolyte [5]	268.1-286.9	15 25	1100 200
Gelatin hydrogel +NaCl [27]	58.8-60.8	----	----
Nanotubes + polyaniline (PANI)+SA [28]	280-442	----	----
PANI + SA + Nanofiber [29]	2093	----	----
Graphene hydrogel films [30]	186	0.61	670
Porous carbon + potassium alginate [31]	279	16.9	----
Carbon nanosheets (GNS) + SA [32]	226.9	65.6	43.75
SA + carbon aerogel [33]	188	10.4	----

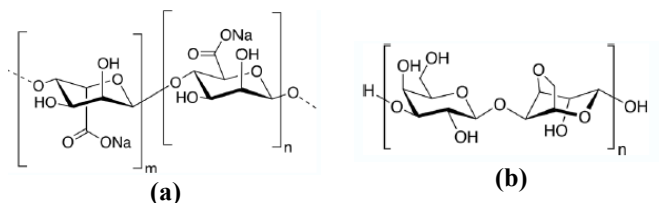


Fig.7. Molecular structures of (a) Sodium alginate (SA) and (b) Agarose

F. Influence of temperature on the supercapacitor performance

The influence of temperature on capacitance and power densities and on the equivalent series resistance is reported in Table II.

For all configurations the capacitance density increases, and the R_{cell} diminishes allowing the increase of power density. Similar behavior is described by [11], and it is there explained by the fact that temperature allows the carbon-carbon bond length expanding, thus, if a portion or all of the micro-pores of carbon nanostructures may open further at higher temperatures and enable access by ions, the observed larger capacitance can

be accounted for. However, further experiments have to be done in order to confirm this hypothesis.

TABLE II
INFLUENCE OF TEMPERATURE ON CAPACITANCE DENSITY, EQUIVALENT SERIES RESISTANCE AND POWER DENSITY

Device	Capacitance density (F/g)		R_{cell} (Ω)		Power density ($W\ kg^{-1}$)	
	15°C	50°C	15°C	50°C	15°C	50°C
Alginate+ CNT (C1)	188.1	205.4	0.35	0.32	1329.9	1435.6
Alginate+ CNT+ DMSO/ Ethanol (C2)	58.0	61.3	0.61	0.57	594.97	636.7
Alginate+ CNT + NaCl (C3)	548.3	603.8	0.30	0.28	1474.82	1579.3

V. CONCLUSION

The good electrochemical performance of a supercapacitor made of a bio-friendly electrolyte loaded with carbon nanotubes was demonstrated.

Additional research has to be done in order to increase the lifetime of the electrolyte; however, it is important to note that the device here depicted has additional advantages such as its simplicity, low-cost and the possibility to fabricate it in a safe manner. Hence, we believe that the biohydrogel-carbon nanotubes based electrolyte may offer attractive prospects validating our approach as a possible route towards all-green, efficient supercapacitor.

ACKNOWLEDGMENT

The authors thank the technical support of F. Ramos, M. Duran and M. Hidalgo and all the members of the Laboratory of Plasma Applications. This work was supported by CONACyT-SENER under Grant 245225 and by the project AM608 ININ.

REFERENCES

[1] Z. Yang, J. Tian, Z. Yin, C. Cui, W. Qian, and F. Wei, "Carbon nanotube- and graphene-based nanomaterials and applications in high-voltage supercapacitor: A review", *Carbon*, vol. 141, pp. 467-480, Jan. 2019.

[2] C. Zhong, Y. Deng, W. Hu, J. Qiao, L. Zhang, and J. Zhang, "A review of electrolyte materials and compositions for electrochemical supercapacitors", *Chem. Soc. Rev.*, vol. 44, no. 21, pp. 7484-7539, Jun. 2015.

[3] J. Galvao, B. Davis, M. Tilley, E. Normando, M.R. Duchon, and M. F. Cordeiro, "Unexpected low-dose toxicity of the universal solvent DMSO" *FASEB J.*, vol. 28, no. 3, pp. 1317-1330, March 2014.

[4] N. Nanbu, T.Ebina, H. Uno, S. Ishizawa, and Y. Sasaki, "Physical and electrochemical properties of quaternary ammonium bis (oxalato) borates and their application to electric double-layer capacitors". *Electrochimica acta*, vol. 52, no. 4, pp. 1763-1770. Dec. 2006.

[5] W. G. Moon, G. P. Kim, M. Lee, H. D. Song, and J. Yi, "A biodegradable gel electrolyte for use in high-performance flexible supercapacitors", *ACS Appl. Mat. & Interfaces*, vol. 7, no. 6, pp. 3503-3511, Jan. 2015.

[6] H. Sun, X.Fu, S. Xie, Y. Jiang, and H. Peng, "Electrochemical capacitors with high output voltages that mimic electric eels", *Adv. Mat.*, vol. 28, no. 10, pp. 2070-2076, Jan 2016.

[7] E. Armelin, M. M. Pérez-Madrugal, C. Alemán, and D. D. Díaz, "Current status and challenges of biohydrogels for applications as supercapacitors and secondary batteries", *J. Mat.Chem. A*, vol. 4, no. 23, pp. 8952-8968, May 2016.

[8] T. B. Schroeder, A. Guha, A. Lamoureux, G. VanRenterghem, D. Sept, M. Shtein, J. Yang, and M. Mayer, "An electric-eel-inspired soft power source from stacked hydrogels". *Nature*, vo. 552, no. 7684, pp. 214-218, Dec. 2017..

[9] I. Kovalenko, B. Zdyrko, A. Magasinski, B. Hertzberg, Z. Milicev, R. Burtovyy, I. Luzinov, and G. Yushin, "A major constituent of brown algae for use in high-capacity Li-ion batteries", *Science*, vol. 334, no. 6052, pp.75-79, Oct. 2011.

[10] C. Louime, J. Fortune, and G. Gervais, "Sargassum invasion of coastal environments: a growing concern". *Am. J. Environm. Sci.*, vol. 13, no. 1, pp. 58-64, Feb. 2017.

[11] Chae, J. H., & Chen, G. Z. (2014). Influences of ions and temperature on performance of carbon nano-particulates in supercapacitors with neutral aqueous electrolytes. *Particuology*, 15, 9-17.

[12] P. Vilchis, M. Pacheco, J. Pacheco, R. Valdivia, C. E. Barrera, P. Balderas, "Synthesis of Boron-Doped Carbon Nanotubes With DC Electric Arc Discharge," in *IEEE Transactions on Plasma Science*, vol.46, no. 8, pp. 3139-3144, Aug. 2018. doi: 10.1109/TPS.2018.2850221

[13] Technical Bulletin "Kelco Algin: hydrophilic derivatives of alginic acid", 2nd ed. Kelco, San Diego, Cal, 25, 1979.

[14] H. S. Kim, "A kinetic study on calcium alginate bead formation". *Kor. J. Chem. Eng.*, vol. 7, no. 1, pp. 1-6, Jan. 1990.

[15] M. D. Stoller, and R. S. Ruoff, "Best practice methods for determining an electrode material's performance for ultracapacitors". *Energy & Env. Sci.*, vol. 3, no. 9, pp.1294-1301, Sept. 2010.

[16] J. W. Campos, M. Beidaghi, K. B. Hatzell, C. R. Dennison, B. Musci, V. Presser, E. Kumbur, and Y. Gogotsi, "Investigation of carbon materials for use as a flowable electrode in electrochemical flow capacitors", *Electrochimica Acta*, vol. 98, pp. 123-130, May 2013.

[17] R. Kötz, and M. J. Carlen, "Principles and applications of electrochemical capacitors", *Electrochimica acta*, vol. 45, no. 15-16, pp. 2483-2498, May 2000.

[18] L. Shi, and M.L. Crow, M. L, "Comparison of ultracapacitor electric circuit models", presented at the *IEEE Power and Energy Society General Meeting-Conversion and Delivery of Electrical Energy in the 21st Century*, Penssylvania, USA, Jul. 1-6, 2008.

[19] L. H. Olesen, M. Z. Bazant, and H. Bruus, "Strongly nonlinear dynamics of electrolytes in large ac voltages". *Phys. Rev. E*, vol. 82, no. 1, 011501, Jul. 2010.

[20] B. A. Mei, O. Munteshari, J. Lau, B. Dunn, and L. Pilon, "Physical interpretations of Nyquist plots for EDLC electrodes and devices". *J. of Phys. Chem. C*, vol. 122, no. 1, pp. 194-206, Dec. 2017.

[21] A. D. Jagadale, V. S. Jamadade, S. N. Pusawale, and C. D. Lokhande, "Effect of scan rate on the morphology of potentiodynamically deposited β -Co(OH)₂ and corresponding supercapacitive performance", *Electrochimica Acta*, vol. 78, pp. 92-97. Sep. 2012.

[22] G. A. Ali, M. M. Yusoff, E. R. Shaaban, and K. F. Chong, "High performance MnO₂ nanoflower supercapacitor electrode by electrochemical recycling of spent batteries". *Ceramics Internat.*, vol. 43, no. 11, pp. 8440-8448, Aug. 2017.

[23] N. A. Choudhury, S. Sampath, and A. K. Shukla, "Gelatin hydrogel electrolytes and their application to electrochemical supercapacitors", *J. Electrochem. Soc.*, vol. 155, no. 1, pp. A74-A81, Jan. 2008.

[24] Mitra, S., Shukla, A. K., & Sampath, S. (2001). Electrochemical capacitors with plasticized gel-polymer electrolytes. *Journal of power sources*, 101(2), 213-218.

[25] L. Niu, Q. Li, F. Wei, X. Chen, and H. Wang, "Electrochemical impedance and morphological characterization of platinum-modified

polyaniline film electrodes and their electrocatalytic activity for methanol oxidation”, *J. Electroanalytical Chem.*, vol. 544, pp. 121-128. March 2003.

- [26] G. Wu, Y. S. Chen, and B. Q. Xu, “Remarkable support effect of SWNTs in Pt catalyst for methanol electrooxidation”, *Electrochem. Comm.*, vol. 7, no. 12, pp. 1237-1243, Dec. 2005.
- [27] W. Wu, Y. Li, L. Yang, Y. Ma, X. Yan, “Preparation and characterization of coaxial multiwalled carbon nanotubes/polyaniline tubular nanocomposites for electrochemical energy storage in the presence of sodium alginate”, *Synth. Metals*, vol. 193, pp. 48-57, July 2014.
- [28] Y. Li, X. Zhao, Q. Xu, Q. Zhang, and D. Chen, “Facile preparation and enhanced capacitance of the polyaniline/sodium alginate nanofiber network for supercapacitors”, *Langmuir*, vol. 27, no. 10, pp. 6458-6463, April 2011.
- [29] Y. Xu, Z. Lin, X. Huang, Y. Liu, Y. Huang, and X. Duan, “Flexible solid-state supercapacitors based on three-dimensional graphene hydrogel films”, *ACS nano*, vol. 7, no. 5, pp. 4042-4049, April 2013.
- [30] S. Sun, B. Ding, R. Liu, and X. Wu, “Facile synthesis of three-dimensional interconnected porous carbon derived from potassium alginate for high performance supercapacitor”, *J. Alloys and Compounds*, vol. 803, pp. 401-406. Sep. 2019.
- [31] D. Wang, J. Nai, L. Xu, T. Sun, “Gunpowder chemistry-assisted exfoliation approach for the synthesis of porous carbon nanosheets for high-performance ionic liquid based supercapacitors”, *J. Energy Storage*, vol. 24, pp. 100764, Aug. 2019.
- [32] B. Wang, D. Li, M. Tang, H. Ma, Y. Gui, X. Tian, F. Quan, X. Song, and Y. Xia, “Alginate-based hierarchical porous carbon aerogel for high-performance supercapacitors. *J. of Alloys and Compounds*”, vol. 749, pp. 517-522, June 2018.
- [33] J. Yan, T. Wei, B. Shao, Z. Fan, W. Qian, M. Zhang, and F. Wei, “Preparation of a graphene nanosheet/polyaniline composite with high specific capacitance”. *Carbon*, vol. 48, no. 2, pp. 487-493, Feb. 2010.
- [34] H. Huang, X. Zeng, W. Li, H. Wang, Q. Wang, Y. Yang, “Reinforced conducting hydrogels prepared from the in situ polymerization of aniline in an aqueous solution of sodium alginate”. *J. Mat. Chem. A*, vol. 2, no. 39, pp. 16516-16522, Aug. 2014.
- [35] Bichat, M. P., Raymundo-Piero, E., & Béguin, F. (2010). High voltage supercapacitor built with seaweed carbons in neutral aqueous electrolyte. *Carbon*, 48,4351-4361.



Marquidia Pacheco was born in Mexico City. She became a Member of IEEE in 2017. She received her B.Sc. in Chemical Engineering in 1996 from the Institute of Technology of Toluca, Mexico. In 1998 and 2003 she obtained her M.Sc. and Ph.D. degrees from the Paul Sabatier

University of Toulouse, France in Physics and Engineering of Plasmas. She works at the ININ, Mexico, on plasma technologies for environmental applications and materials to store energy. She obtained the Silver Medal in the Week of Science and Innovation 2009 in Mexico City and at the same year the Award granted by UNESCO-L'OREAL 2009 for women in Science. In 2019 she obtained the IEEE NPSS Women in Leadership Development Travel Grant recipient.



María Fernanda Monroy is graduate of Engineering in Sustainable Energetic Systems of the Universidad Autónoma del Estado de México. During her career, she participated to disseminate the Science and culture. She developed the Eng. thesis

"Design of a supercapacitor consisting of carbon nanotubes and a working electrolyte based on sodium compounds" at the Instituto Nacional de Investigaciones Nucleares. Currently, she is coordinator of the energy area in the company Xbab, Energy and Sustainability.



Alfredo SANTANA-DÍAZ has a BS in Electronic and Control Systems Engineer from ITESM (93), a Master in Manufacturing Systems from ITESM (96), and a Master in Control and Science Computer from Paul Sabatier Université (1999). He has a PhD in Control and Systems from Paul Sabatier Université (2003); his research work was developed at

LAAS-CNRS, applied to driver's impairment detection using wavelets and statistical learning.

Since May 2003 he works at ITESM Campus Toluca. Currently, he is a Full Professor and collaborates at the Research Center in Automotive Mechatronics of ITESM Campus Toluca in subjects concerning environment and energy consumption for vehicles.



Joel Pacheco received the B.Sc. degree in Industrial Electronics and the M.Sc. degree in Power Electronics from the Chihuahua Institute of Technology, México, in 1974 and 1983, respectively, and the DEA and Ph.D. degrees in electronics from the National Polytechnic Institute of Toulouse,

France in 1993. Since 1974 he has been with the Mexican National Institute of Nuclear Research (ININ) where he has worked in several research and development projects related with thermal and non-thermal plasmas, electrical discharges and pollution control. He is member of the National System of Researchers in Mexico since 1989. He joined the Toluca Institute of Technology in 1987, where he is currently Professor of Power Electronics. Since 1995 he has been responsible for the development and applications of the Thermal Plasma Laboratory at ININ.



Ricardo Valdivia-Barrientos was born in Mexico City, Mexico. He received the B.S. and Ph.D. degrees in electronics engineering from the Institute of Technology of Toluca, Mexico, in 2003 and 2008, respectively. He has worked in the development of power supply systems and associated electronic devices for

plasma sources with the Plasma Applications Laboratory, National Institute of Nuclear Research, Mexico, since 2008. His current research interests include plasma processing of materials, electronic instrumentation, plasma modeling and simulation, control systems, and plasma diagnostics.



Xin Tu (M'12-SM'15) was born in Ningbo, China on 20th April 1978. He received the Ph.D. degree in physics from the University of Rouen (CORIA – CNRS UMR 6614), Rouen, France, in 2006 and the Ph.D. degree in thermal engineering from Zhejiang University, Hangzhou, China, in 2007.

He is Professor at the Department of Electrical Engineering and Electronics at the University of Liverpool. Dr. Tu has published over 80 papers in international journals and given over 20 invited talks. In 2014, he received a prestigious B. Eliasson Award from the International Symposium on Plasmas for Catalysts and Energy Materials to recognise his contributions to plasma-catalysis with emphasis on the fundamental understanding of the synergy of plasma-catalysis and nanomaterial formation in plasma.



J. Alberto Gonzalez-Pedroza is graduate of Engineering in Mechatronics from The Instituto Tecnológico de Toluca, Mexico. He developed the project to obtain his Eng. Degree: Electrochemical characterization of a carbon nanotubes supercapacitor.



María Teresa Ramírez-Palma has a BS in Chemistry (UAEMéx, 2004), a Master in Science and Engineering of Materials (UNAM, 2010), a PhD in Chemistry (UAEMéx, 2017) and a Postdoctoral training (ININ, 2017). She worked at AGA Gas, as chemical analyst and had training for EPA gas analysis in Ohio at the USA

AGA Gas plant, (Linde group), then she worked at Polioles, (BASF México group), as project engineer in the development of new products for petrochemical industry. Since 2015, she works at the UAEMéx as a professor at the Engineering Faculty where she has been working in nanomaterials applied to energy